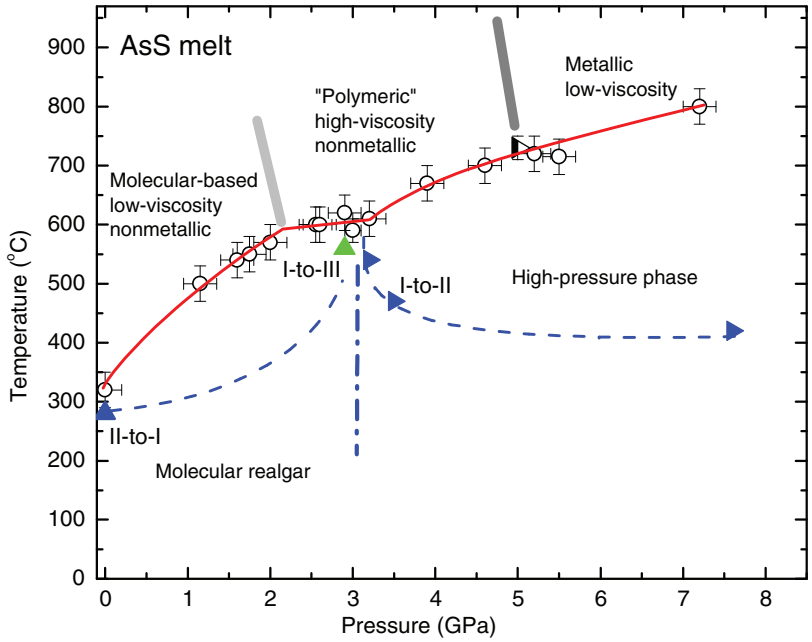

Figure 2.3. Pressure–temperature phase diagram of AsS in crystalline and liquid states. Opened circles correspond to the experimental melting points of AsS crystal, while the thin line and thick lines are approximations of melting line and boundaries between liquid states, respectively. Solid triangles correspond to phase transitions between crystalline phases, determined at the near isobaric heating. Semisolid triangle corresponds to metallization of liquid AsS. Dashed lines are approximation of experimental transition lines (kinetically dependent) from AsS I (right line) and AsS II (left line) crystalline phases, while dashed-dotted line is approximation of I–II equilibrium line.

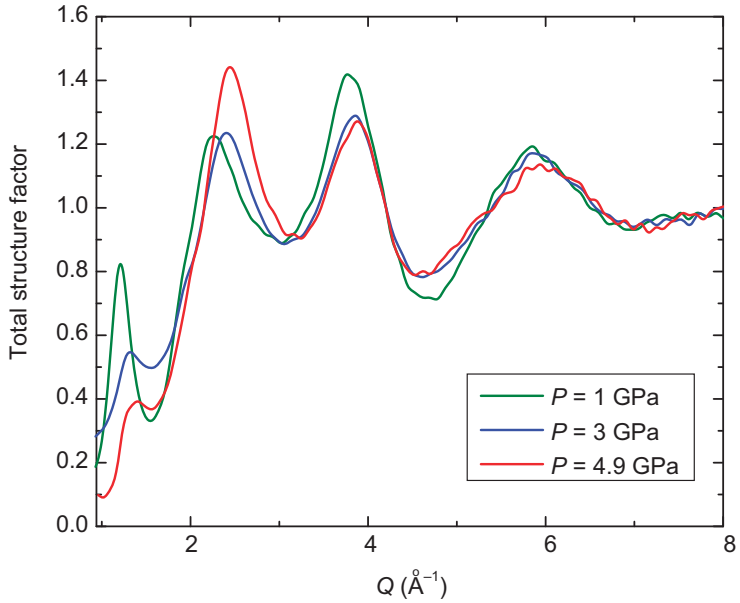

Figure 2.4. Typical structure factors for different states of the AsS melt, including the molecular liquid at 1 GPa, polymeric liquid at 3 GPa, and metallic liquid at 4.9 GPa. All structure factors are obtained for the experimental sets of spectra recorded at temperatures exceeding the melting point by 70K.

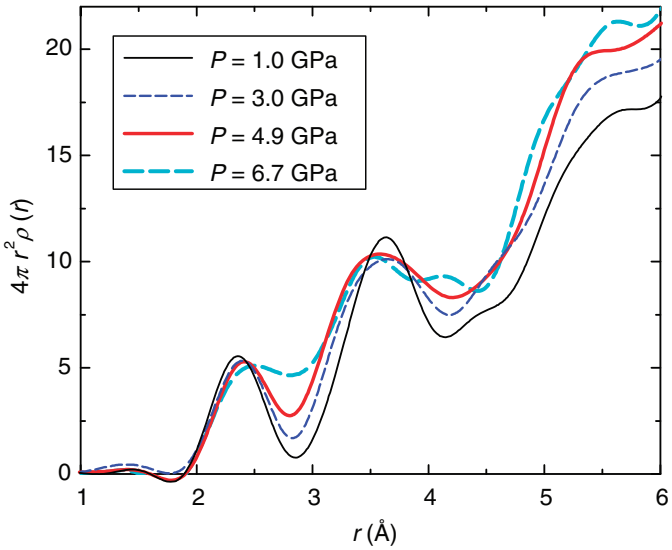

Figure 2.5. Radial distribution functions of the AsS melt at different pressures.

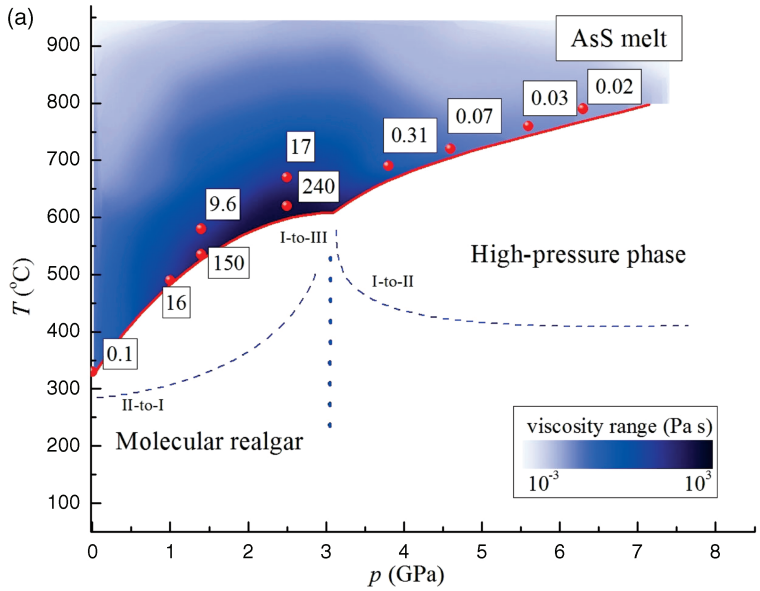

Figure 2.6. Viscosity of the AsS melt under pressure: (**a**) liquid viscosity values mapped onto the pressure–temperature phase diagram of AsS (in Pa s units); (**b**) viscosity versus pressure dependence of the liquid AsS along the melting curve.

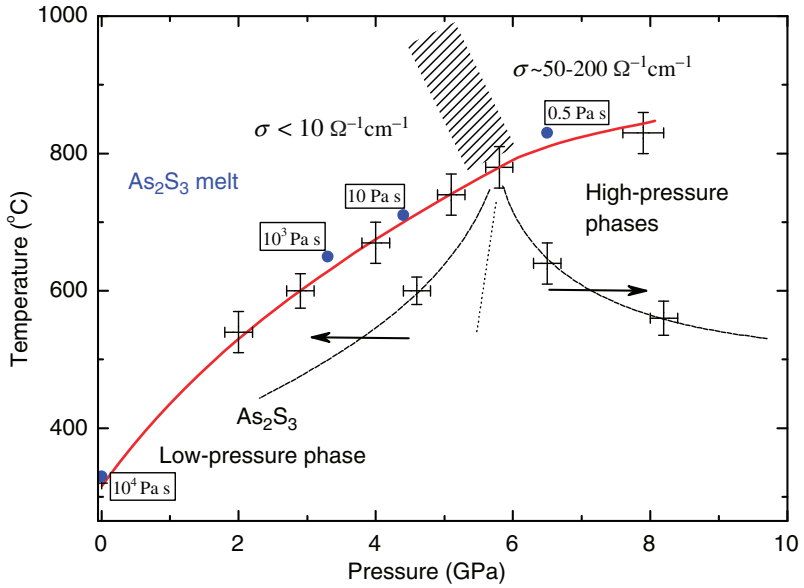

Figure 2.7. Experimental pressure–temperature phase diagram of As_2S_3. Crosses show points and their uncertainties for the experimentally observed phase transitions. Solid line is an approximation of the melting curve, and dashed lines are approximations for the experimental kinetic curves of the solid–solid phase transitions. The points of viscosity measurements are shown by solid circles and marked by measured values of viscosity (in Pa s units). Shaded region selects a boundary between the melting states with low and high conductivities.

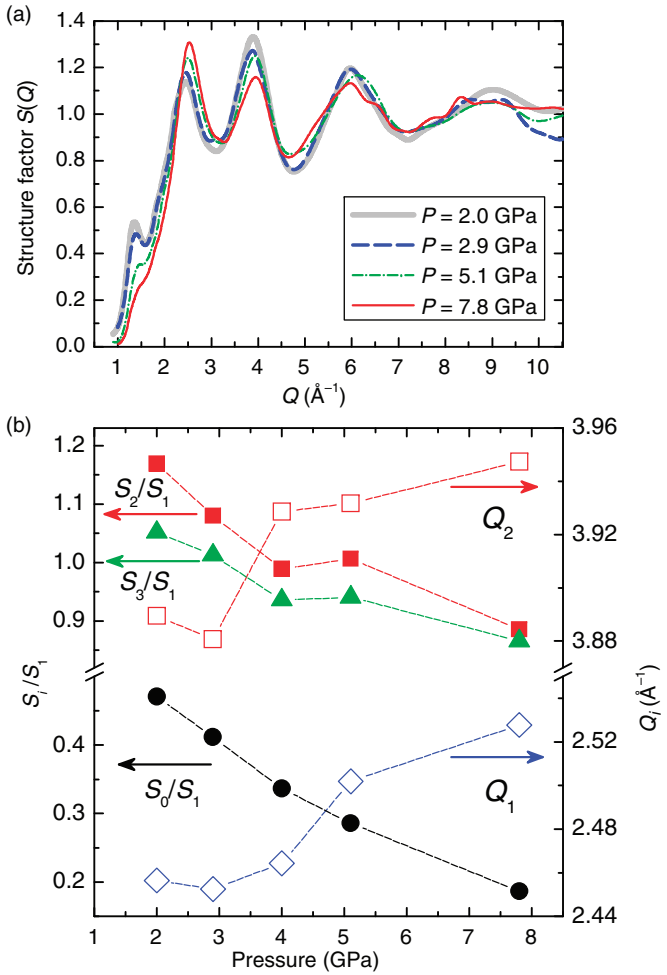

Figure 2.8. Calculated from the experimental EDXD data and smoothed total interference functions (structure factors) of the As_2S_3 melt at different pressures near melting curve (**a**); Q-positions of the first and second main peaks of the structure factor $S(Q)$, as well as amplitudes of the prepeak, second and third peaks of $S(Q)$ scaled by the amplitude of the first main peak (**b**). Dashed lines on the panel (b) are guides for eyes.

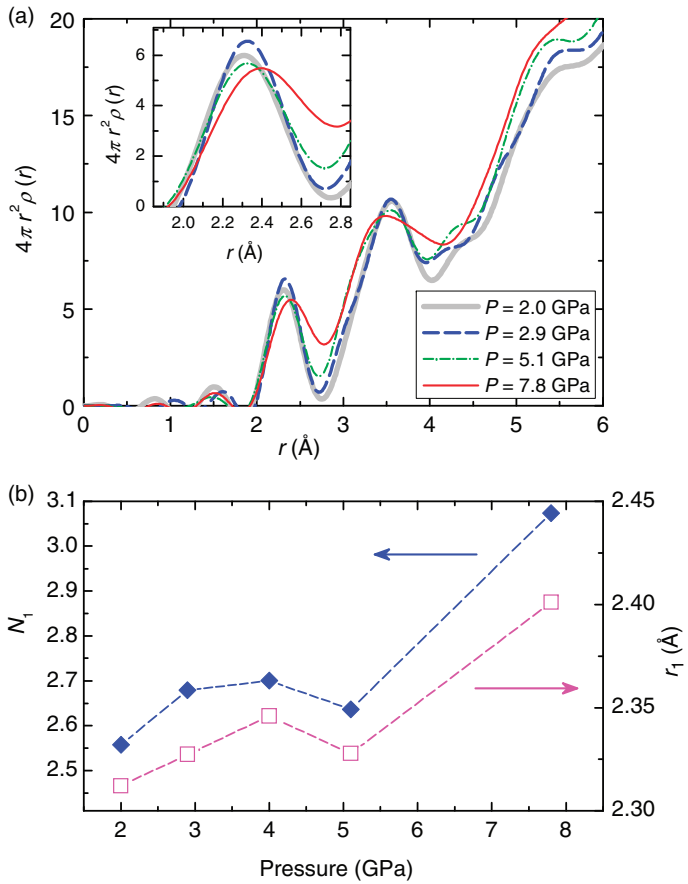

Figure 2.9. Radial distribution functions of the As_2S_3 melt (**a**), where the inset shows the same for the first coordination sphere; pressure dependence of the radius r_1 and area under the radial distribution curve N_1 for the first coordination sphere (**b**). Dashed lines on the panel (b) are guides for eyes.

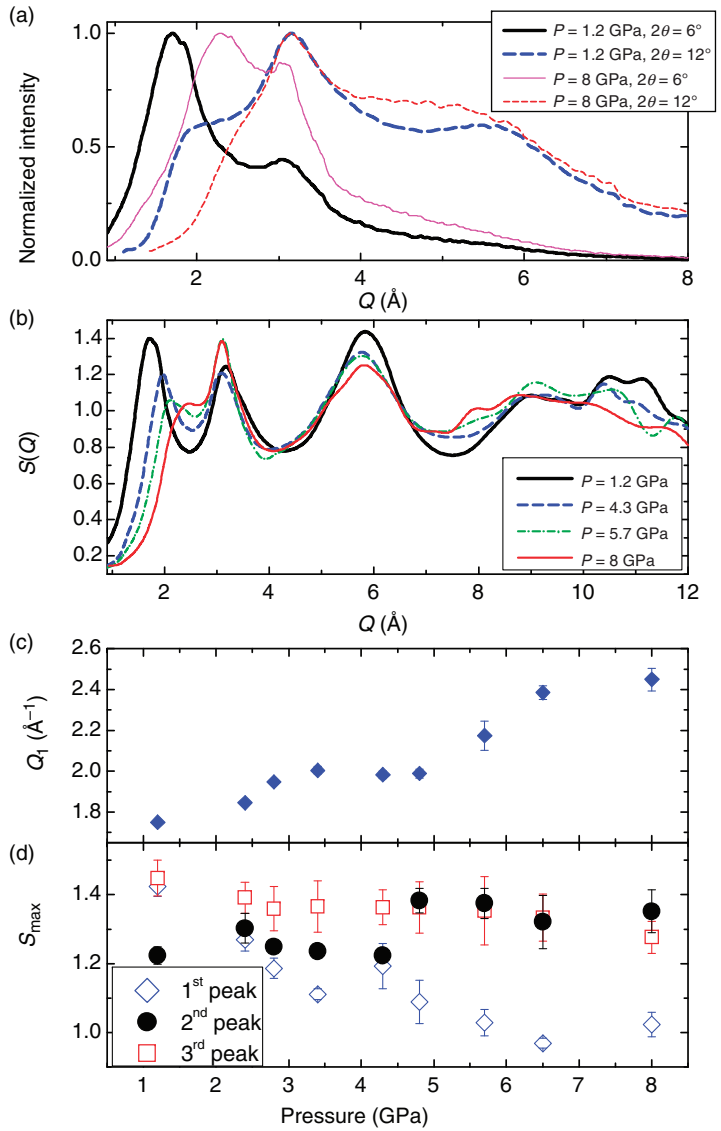

Figure 2.10. Examples of the EDXD data for the liquid B_2O_3 under pressure (**a**), measured at the two angles of the detector; calculated from the experimental EDXD data and smoothed total interference functions for different pressures (**b**); Q-position of the first peak of the structure factor (**c**); and amplitudes of the first three maxima of the structure factor (**d**).

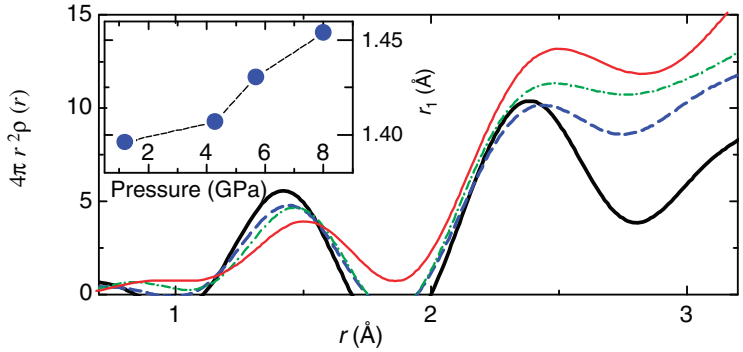

Figure 2.11. Radial distribution functions for the liquid B_2O_3 under pressure, where the inset shows the pressure dependence of the radius of the first coordination sphere.

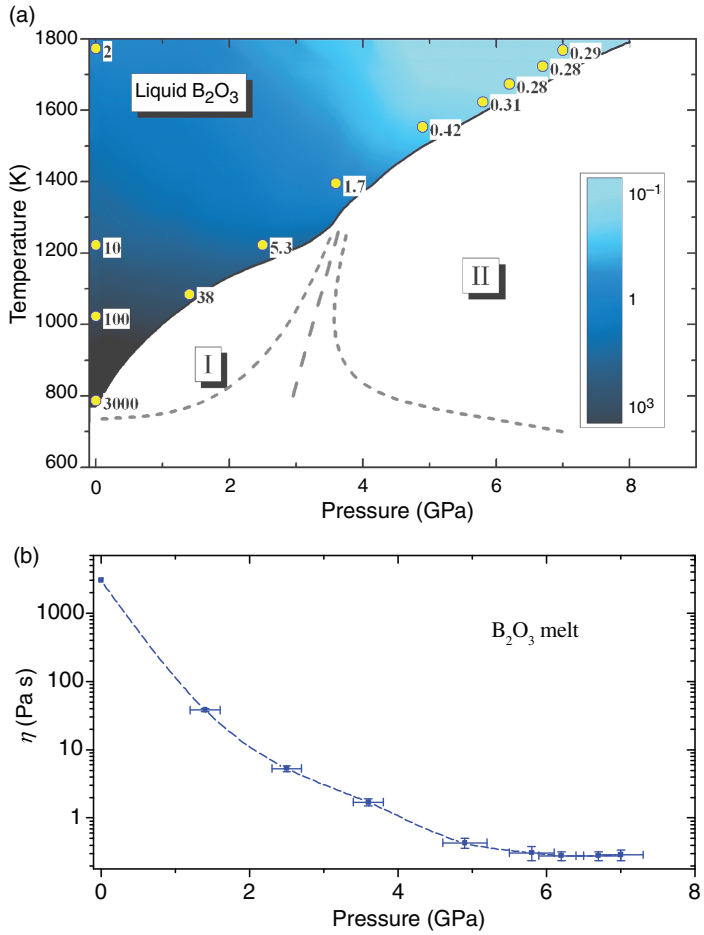

Figure 2.12. Experimental phase diagram of B_2O_3 with the approximated color mapping of the melt viscosity (in Pa s units) (**a**) and pressure dependence of viscosity along the melting curve (**b**). The experimental pressure–temperature points, where viscosity was measured, are marked on the panel (a) by the measured values of viscosity.